Available online at www.sciencedirect.com
SCIENCE DIRECT®
Advances in Water Resources 27 (2004) 815–830
Advances in Water Resources
www.elsevier.com/locate/advwatres

Methods for generating non-separable spatiotemporal covariance models with potential environmental applications

A. Kolovos [a], G. Christakos [a,*], D.T. Hristopulos [b], M.L. Serre [a]

[a] *Center for the Integrated Study of the Environment (CISE), Department of Environmental Science and Engineering, University of North Carolina at Chapel Hill, 111 Rosenau Hall, Chapel Hill, NC 27599-7431, USA*
[b] *Department of Mineral Resources Engineering, Technical University of Crete, Chania, Crete, Greece*

Received 18 November 2003; received in revised form 2 March 2004; accepted 30 April 2004

Abstract

Environmental processes (e.g., groundwater contaminants, air pollution patterns, air–water and air–soil energy exchanges) are characterized by variability and uncertainty. Spatiotemporal random fields are used to represent correlations between fluctuations in the composite space–time domain. Modelling the effects of fluctuations with suitable covariance functions can improve our ability to characterize and predict space–time variations in various natural systems (e.g., environmental media, long-term climatic evolutions on local/global scales, and human exposure to pollutants). The goal of this work is to present the reader with various methods for constructing space–time covariance models. In this context, we provide a mathematical exposition and visual representations of several theoretical covariance models. These include non-separable (in space and time) covariance models derived from physical laws (i.e., differential equations and dynamic rules), spectral functions, and generalized random fields. It is also shown that non-separability is often a direct result of the physical laws that govern the process. The proposed methods can generate covariance models for homogeneous/stationary as well as for non-homogeneous/non-stationary environmental processes across space and time. We investigate several properties (short-range and asymptotic behavior, shape of the covariance function etc.) of these models and present plots of the space–time dependence for various parameter values.

Keywords: Spatiotemporal: Environmental processes: Random fields: Stochastics: Statistics: Geostatistics

1. Introduction

The vast majority of environmental processes (e.g., flow and transport distributions, pollutant trends, and soil–air–water energy exchanges) are characterized by significant variability and uncertainty that result from ontologic factors and epistemic limitations. The former are due to the inherent complexity of the natural systems, whereas the latter are associated with incomplete information (e.g., resulting from an inability to collect enough data, poor understanding of the underlying mechanisms, limited computational capabilities and numerical errors). Classical statistics approaches often fail to provide a sufficient description of a process' evolution across space and time, which makes it necessary to model it in terms of the *spatiotemporal random field* (S/TRF) theory, ordinary or generalized. The S/TRF theory accounts for the fact that the physical laws affect both the mean and the space–time covariance function of the associated environmental processes. For example, in hydrologic modelling the covariance of the hydraulic head is related to the covariance of the hydraulic conductivity by means of an equation determined from

* Corresponding author. Tel.: +1 919 966 1767; fax: +1 919 966 7911.
E-mail address: george_christakos@unc.edu (G. Christakos).

0309-1708/$ - see front matter
doi:10.1016/j.advwatres.2004.04.002

the respective physical laws (i.e., Darcy's law and continuity equation; see, e.g., [34].

Let $X(\boldsymbol{p})$ be a S/TRF, where $\boldsymbol{p} = (\boldsymbol{s}, t) \in R^n \times T(T \subset R^1)$; the vector $\boldsymbol{s}$ denotes spatial location in the n-dimensional Euclidean space R^n and the scalar t denotes time along the axis T. The S/TRF theory distinguishes between two major groups of *spatiotemporal covariance functions*, as follows (for a detailed presentation of the S/TRF theory see, [7,8,12]):

- The group of *ordinary* covariance functions, denoted by c_X. The ordinary centered covariance function is defined by $c_X(\boldsymbol{r}, \tau) = \overline{X(\boldsymbol{s}, t)X(\boldsymbol{s}+\boldsymbol{r}, t+\tau)} - \overline{X(\boldsymbol{s}, t)}\,\overline{X(\boldsymbol{s}+\boldsymbol{r}, t+\tau)}$, where the bar denotes stochastic expectation. The ordinary non-centered covariance function is defined as $C_X(\boldsymbol{r}, \tau) = \overline{X(\boldsymbol{s}, t)X(\boldsymbol{s}+\boldsymbol{r}, t+\tau)}$. The centered covariance provides explicit expressions of the correlations, whereas the non-centered covariance also includes information about the trend dependence that control the distribution of the natural process $X(\boldsymbol{p})$. In theoretical investigations and applied geostatistical analyses the ordinary covariance functions are often considered to represent space homogeneous/time stationary S/TRF, in which case they are functions only of the space and time distances, $\boldsymbol{r} = \boldsymbol{s}' - \boldsymbol{s}$ and $\tau = t' - t$, respectively, between any pair of points $\boldsymbol{p} = (\boldsymbol{s}, t)$ and $\boldsymbol{p}' = (\boldsymbol{s}', t')$. If the random field is space homogeneous/time stationary, and if $c_X(\boldsymbol{r}, \tau) = c_X(r = \|\boldsymbol{r}\|, \tau)$, where $\|\boldsymbol{r}\|$ is the magnitude of the spatial distance vector $\boldsymbol{r}$, the field is spatially isotropic in the weak sense (sometimes referred to as second-order isotropy, as well). If the two points are considered at the same instant in time, a weaker condition that defines spatial isotropy is $c_X(\boldsymbol{r}, 0) = c_X(r = \|\boldsymbol{r}\|, 0)$. The $c_X(\boldsymbol{r}, \tau)$ often (although not necessarily) tends asymptotically to zero, unless it is different from zero only within a bounded interval and becomes equal to zero outside this interval (e.g., the spherical model). If the covariance function is integrable in space or time, it has a finite correlation range in the respective domain. The covariance spectral density, $\tilde{c}_X(\boldsymbol{k}, \omega)$, is the Fourier transform of the covariance function in the frequency domain (see Appendix). In the this domain, the vector $\boldsymbol{k}$ represents the spatial frequency (wave-vector), and ω the time frequency.
- The group of *generalized* covariance functions, denoted by κ_X, are linked with generalized S/TRF which are used to represent non-homogeneous/non-stationary natural patterns, physical coarse graining, and multiscale processes. Fractals and wavelets are special cases of the generalized S/TRF theory. The generalized covariances behave differently than the ordinary ones, because they are derived from functional linear representations of the original random field $X(\boldsymbol{p})$. The field's degree of departure from homogeneity/stationarity is expressed by means of the space and time continuity orders. The behavior of the covariance at large distance is not necessarily decreasing and, thus, correlation ranges are not defined. *Permissibility* criteria are mathematical conditions that a function must satisfy in order to be a permissible covariance model, of the ordinary or the generalized kind. An extensive list of covariance permissibility criteria is available, depending on the random field type, e.g., homogeneous vs. non-homogeneous, stationary vs. non-stationary [4,8,12]. As is discussed in these references, in the case of homogeneous/stationary random fields, many of the permissibility criteria are a direct consequence of Bochner's theorem: a function is a permissible covariance model if and only if its spectral density is non-negative and the integral of the spectral density over all frequencies is bounded (see also the following section). In the case of non-homogeneous/non-stationary fields, a suitable mathematical extension of Bochner's theorem is required (see references above).

The covariance function is *separable* if it can be decomposed into components (e.g., by means of a product or a sum) with purely spatial or temporal dependence, and *non-separable* if such a decomposition is not possible. For example, separable ordinary covariance functions can have the general form $c_X(\boldsymbol{s}, t; \boldsymbol{s}', t') = c_{X(1)}(\boldsymbol{s}, \boldsymbol{s}')c_{X(2)}(t, t')$, where $c_{X(1)}(\boldsymbol{s}, \boldsymbol{s}')$ is a purely spatial and $c_{X(2)}(t, t')$ a purely temporal covariance. Separable models of space–time covariance functions are valuable in both physical and health applications (e.g., [2, p. 51–59;12, p. 102–109 and 163–170;26, p. 664–666]). However, in many cases non-separable models are physically more realistic. Several theoretical models of non-separable covariances can be found: (a) in the *spatiotemporal stochastics* literature [2,3,7–15,19,37]; as well as (b) in the *statistics* literature [16,18,20,27–30,33,36]. Covariance models of the group a above can be generated from partial differential equations representing physical laws, construction of permissible spectral densities, dynamic rules (e.g., algorithmically tractable physical models of growth that cannot be expressed in terms of differential equations), generalized random fields, etc. In this work we investigate covariance models of the group a, and provide appropriate visualizations of some of their most important features across space and time.

2. Non-separable spatiotemporal covariance models

The non-separable covariance models that we investigate below include spatially homogeneous/temporally stationary as well as non-homogeneous/non-stationary S/TRF (including generalized and fractal models, see also Section 2.3 below). We study the main characteristics of these models as well as their space–time behavior for several combinations of their parameters.

Before continuing with the classes of non-separable covariance models, we discuss *space transformation* operators that permit constructing covariance models in two and three dimensions from one-dimensional models. In particular, [4,6] introduced space transformation operators, which were later applied to various problems (see [12], for a detailed review of the relevant literature). The classical Radon theory (Radon, 1917; [35]) provides a general formulation for deriving space transformation operators (e.g., the geostatistical turning bands method is a special case of the Radon theory). One space transformation operator links a covariance model, $c_{X,1}$, in $R^1 \times T$ with covariance models, $c_{X,n}$, in $R^n \times T$ ($n = 2, 3$) by means of the integral relation

$$c_{X,n}(r,\tau) = E_n \int_0^1 \mathrm{d}u(1-u^2)^{(n-1)/2} c_{X,1}(ur,\tau), \tag{1}$$

where $E_n = 2\Gamma(n)/(\sqrt{\pi}\Gamma[(n-1)/2])$, Γ is the gamma function, and $r = \|\boldsymbol{r}\|$ is a scalar that refers to the magnitude of the lag vector $\boldsymbol{r}$. Space transformation implies that if a permissible covariance model is available in $R^1 \times T$, new models can be derived in $R^n \times T$ (possibly geometrically anisotropic after an appropriate change of variables) by means of Eq. (1). The space transformation approach can be used in the frequency domain, as well. Indeed, another space transformation operator relates the spectral density $\tilde{c}_{X,1}$ of the covariance function $c_{X,1}$ (in $R^1 \times T$) with the spectral densities $\tilde{c}_{X,n}$ of $c_{X,n}$ (in $R^n \times T$; $n = 2, 3$) by means of the following equation

$$\tilde{c}_{X,n}(k,\omega) = \begin{cases} \int_k^\infty \mathrm{d}u(u^2-k^2)^{1/2} & \\ \quad \times \frac{\mathrm{d}}{\mathrm{d}u}[u^{-1}\frac{\mathrm{d}}{\mathrm{d}u}\tilde{c}_{X,1}(u,\omega)] & \text{for} \quad n=2, \\ -(1/2\pi)k^{-1}\frac{\mathrm{d}}{\mathrm{d}k}\tilde{c}_{X,1}(k,\omega) & \text{for} \quad n=3, \end{cases} \tag{2}$$

where the scalar k is the magnitude of the space–frequency vector $\boldsymbol{k}$. Eqs. (1) and (2) above are instrumental in developing new classes of non-separable covariance models in space–time. In light of Bochner's theorem, given a covariance model $c_{X,1}$ that is permissible in $R^1 \times T$, one can examine the permissibility of the same function in $R^n \times T$ by deriving its spectral density $\tilde{c}_{X,n}$ from Eq. (2) above, and then testing if the requirements of the Bochner theorem are satisfied for the obtained function. The same space transformation approach as above applies in the case of generalized covariance models [4, p. 258]. Useful expressions analogous to the Eqs. (1) and (2) can be derived in terms of different combinations of space transformation operators in $R^n \times T$.

In addition, any model that is permissible in n dimensions is also permissible in n' dimensions, where $n' < n$. Since permissibility in $n = 3$ implies permissibility in $n = 2$ [4], in some cases it may be more convenient mathematically to investigate the permissibility of a covariance model in $R^3 \times T$, even if the domain of interest is $R^2 \times T$. Note that anisotropic models can be trivially derived from the isotropic ones generated by Eqs. (1) or (2) above. In the case of geometric anisotropy, an anisotropic model can be obtained from an isotropic one by means of a coordinate rotation and rescaling of the axes. Alternatively, the anisotropic parameters can be determined directly from the data using the method proposed in [22,24]. If the coordinates are then transformed by respective rotation and rescaling transformations the process can be modelled by means of an isotropic model.

2.1. Covariance models generated from physical differential equations

Many spatiotemporal covariance models can be derived as solutions of *physical partial differential equations* (pde). Covariance functions that are generated by explicit solutions of governing pde are permissible by construction, so long as all the covariance functions that pertain to the pde inputs (e.g., sources, initial and boundary conditions) are permissible. It should be noticed that the covariance functions are often called *two-point statistics* in the physics and engineering literature because they express physics-based correlations between pairs of points in space–time.

A large class of non-separable covariance models is associated with the *general stochastic* pde, $\partial/\partial t[X(\boldsymbol{p})] = \mathscr{L}_{\boldsymbol{s}}[X(\boldsymbol{p})]$, where $\mathscr{L}_{\boldsymbol{s}}$ is a linear spatial differential operator in $R^n \times T$. This class includes various covariance models, one of which is the family of non-centered covariances given below [12, p. 109–112]

$$C_X(\boldsymbol{s},t;\boldsymbol{s}',t') = \begin{cases} \sum_{j,k=0}^{\infty} c_{jk}\chi_{1j}(\boldsymbol{s})\chi_{1k}(\boldsymbol{s}')\chi_{2j}(t)\chi_{2k}(t'), \\ \sum_{j,k=0}^{\infty} A_jA_kc_{\chi(j,k)}(\boldsymbol{s},\boldsymbol{s}')\chi_{2j}(t)\chi_{2k}(t'), \\ \sum_{j,k=0}^{\infty} \overline{A_jA_k\chi_{1j}(\boldsymbol{s})\chi_{1k}(\boldsymbol{s}')}\chi_{2j}(t)\chi_{2k}(t'), \end{cases} \tag{3a–c}$$

where χ_{1j} and χ_{2j} represent eigenfunctions (modes) of the differential equation. Each mode has an amplitude A_j, which is determined from the boundary and initial conditions. In Eq. (3a) the coefficients c_{ij} represent correlations of the mode coefficients, i.e., they correspond to the ensemble average $c_{jk} = \overline{A_jA_k}$. In Eq. (3b) the function $c_{\chi(j,k)}$ denotes the mode correlation $\overline{\chi_{1j}(\boldsymbol{s})\chi_{1k}(\boldsymbol{s}')}$ and A_j are deterministic mode amplitudes. In (3c) the A_j are random variables to be determined from the boundary and initial conditions (B/IC). Randomness in the covariance models of Eq. (3) can be introduced by: (i) the B/IC leading to random coefficients A_j; (ii) the differential operator $\mathscr{L}_{\boldsymbol{s}}$ leading to random eigenfunctions χ_{1j}; and (iii) by both of the above. Models (3) may be non-homogeneous/non-stationary due to a number of reasons, including the boundary and initial condition effects.

For visualization purposes, a diffusion pde in the $R^1 \times T$ domain is considered with a diffusion coefficient D. The initial condition is a parabolic concentration profile of the length L of the domain, i.e. $f(s) = c_0 4 (s/L)(1 - s/L)^{-1}$, where c_0 is a random variable with

$\overline{c_0^2} = 1$ and L is the domain size. Then, $c_{jk} = \overline{c_0^2} a_j a_k$, $\chi_{1j} = \cos(j\pi s/L)$ and $\chi_{2j} = \exp(-Dj^2\pi^2 t/L^2)$; $a_j = 2/3$ (if $j = 0$), $= -8(j\pi)^{-2} - [1 + (-1)^j]$ (if $j > 0$). By inserting these parameters into Eq. (3a) and letting $L = 1$ we obtained the (non-centered) covariance function $C_X(\mathbf{s}, t; \mathbf{s}', t')$ plotted in Fig. 1. This function depends on the

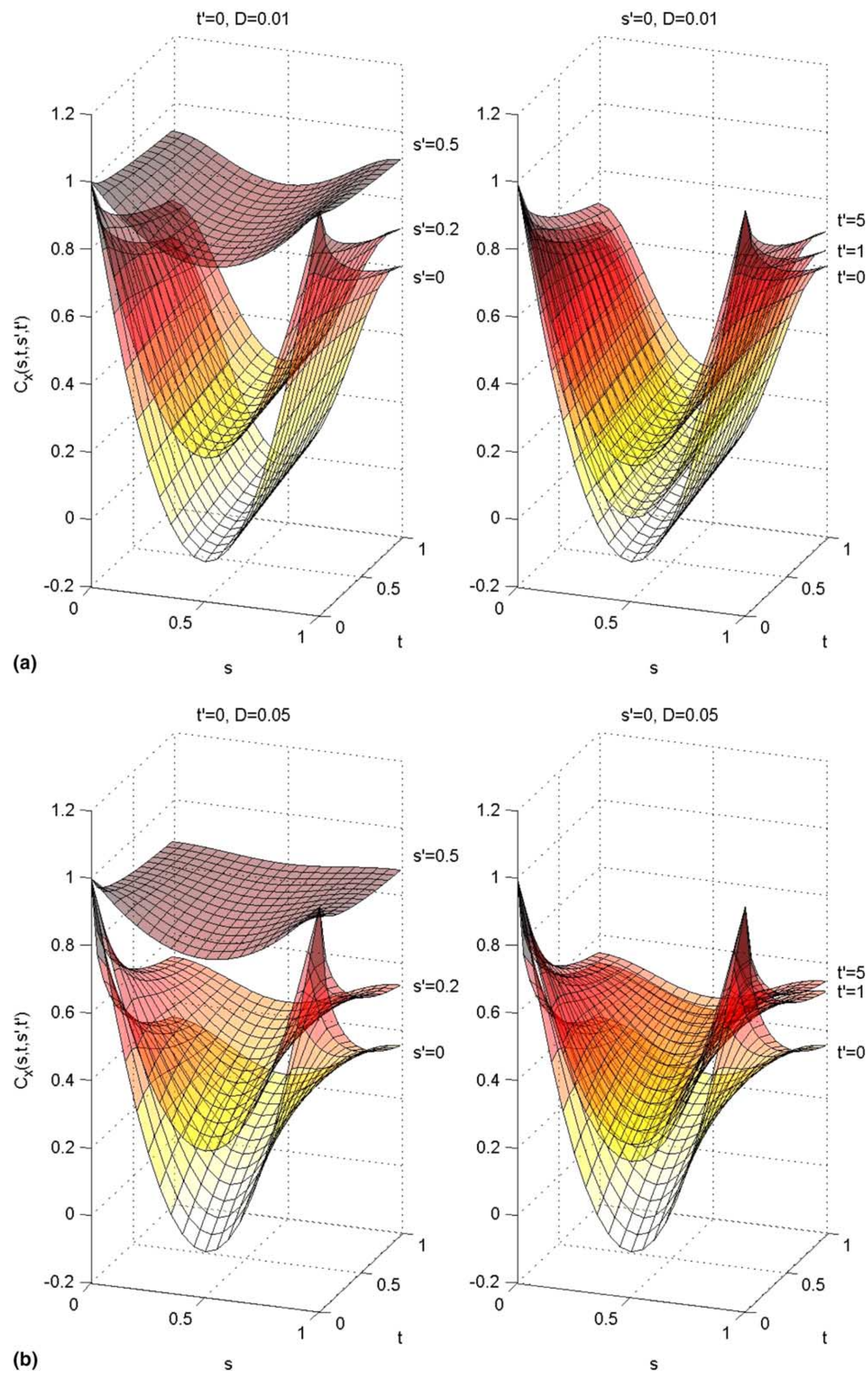

Fig. 1. (a) Plots of the non-separable covariance model of Eq. (3a) for a spatial domain of size $L = 1$ in the $R^1 \times T$ domain. The diffusion coefficient is $D = 0.01$. (b) Plots of the non-separable covariance model of Eq. (3a) for a spatial domain of size $L = 1$ in the $R^1 \times T$ domain. The diffusion coefficient is $D = 0.05$.

space/time coordinates of both points $p = (s, t)$ and $p' = (s', t')$, and not just on the space and time distances between the two points. More specifically, in Fig. 1 we plot the covariance values between points in the (s, t)-domain and the points $(s' = 0, t')$ and $(s', t' = 0)$ throughout the domain. We create these plots for two different values of the coefficient D in Fig. 1a and b. Several other spatiotemporal covariance models can be generated from Eq. (3) using different boundary and initial conditions.

Non-separable covariance models across space and time are obtained from *parabolic* pde, as well. The following non-separable covariance model

$$c_X(r,\tau) = 0.5\Big[\exp(-ar)\mathrm{Erfc}\Big(a\sqrt{c^{-1}\tau} - 0.5r\sqrt{c\tau^{-1}}\Big) + \exp(ar)\mathrm{Erfc}(a\sqrt{c^{-1}\tau} + 0.5r\sqrt{c\tau^{-1}})\Big] \quad (4)$$

is derived from a model initially proposed by Heine [21, p. 170–178]. The a and c are constant coefficients associated with the parabolic pde, and $\mathrm{Erfc}(x)$ is a complementary error function, see Eq. (A.3) of the Appendix. The above model represents spatially homogeneous/temporally stationary fields in $R^1 \times T$. Notice that $c_X \to 2\mathrm{Erfc}(a\sqrt{\tau/c})$ as $r \to 0$; and $c_x \to \sigma^2$ as r, $\tau \to 0$. The model (4) is plotted in Fig. 2 for various choices of the coefficient values a and c. The values of the coefficients affect the ranges and shape of the covariance models. The covariance, e.g., decreases faster for increasing values of the a/c ratio. Another observation is that the covariance declines faster in the spatial than in the temporal direction. Using Eq. (2), it is found that model (4) is permissible for $n = 2$ and 3, as well. Certain extensions of the model (4) were proposed by Ma [29].

Furthermore, new covariance models in $R^n \times T$ ($n > 1$) are derived from model (4) by applying the space transformation of Eq. (1) above, i.e.,

$$c_{X,n}(r,\tau) = 0.5E\int_0^1 \mathrm{d}u(1-u^2)^{(n-1)/2}\Big[\exp(-aur)\mathrm{Erfc}\Big(a\sqrt{c^{-1}\tau} - 0.5ur\sqrt{c\tau^{-1}}\Big) + \exp(aur)\mathrm{Erfc}\Big(a\sqrt{c^{-1}\tau} + 0.5ur\sqrt{c\tau^{-1}}\Big)\Big]. \quad (5)$$

Models (5) are plotted in Fig. 2 for $n = 3$. Space–time plots render the behavior of the covariance model in the entire space–time domain, in contrast with standard practice (e.g., varying r and keeping fixed τ, or vice versa). Consider, e.g., Fig. 2, in which visualizing the covariance model behavior in the composite space–time domain (varying both r and τ) provides better understanding of space–time dependence than simple space or time covariance plots allow.

A non-separable spatiotemporal covariance model in $R^n \times T$ ($n = 1, 2, 3$) inspired from the *diffusion* equation, with several physical applications, is the following [9, p. 226]

$$c_X(r,\tau) \cong (4\alpha\pi\tau)^{-n/2}\exp(-r^2/4\alpha\tau), \quad (6)$$

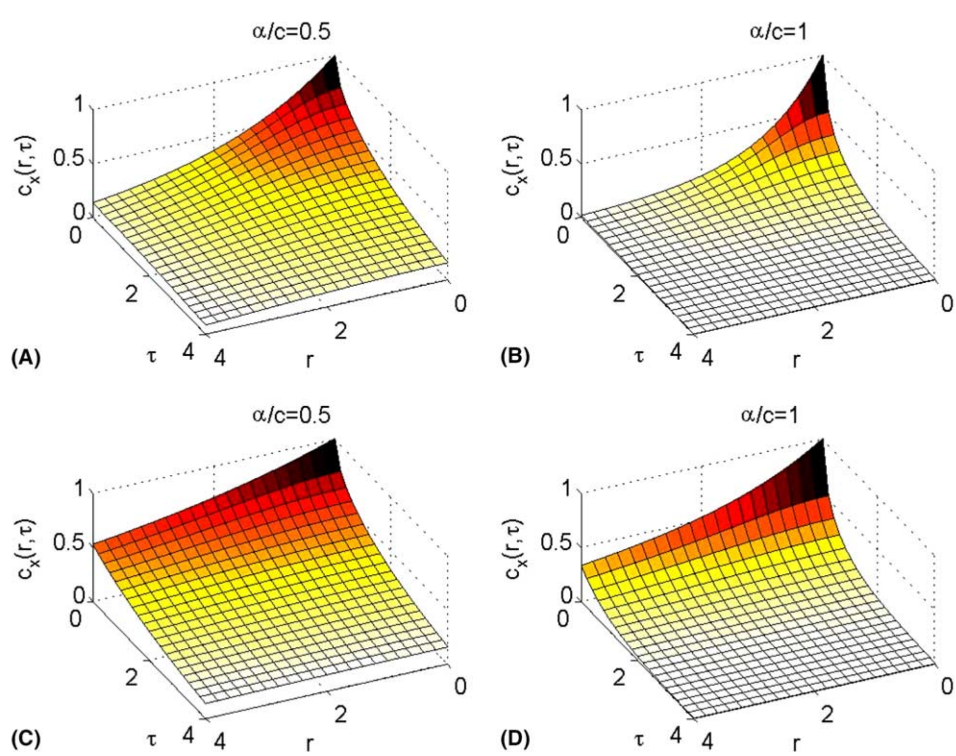

Fig. 2. Plots of the non-separable covariance model of Eq. (4) in the $R^1 \times T$ domain (plots A and B), and of the model in Eq. (5) in the $R^3 \times T$ domain (plots C and D) for various values of the ratio α/c.

where $\alpha > 0$. Note that this model tends to a delta function as $\tau \to 0$. The symbol "$\cong$" denotes that the covariance is of this functional form asymptotically as $r \to \infty$ and $\tau \to \infty$ but not close to the origin. To obtain permissible covariance models, the singularity at zero lag must be tamed, e.g., by means of a short-range cutoff. Short-range cutoffs are related to physical scales of the underlying process [22, p. 45]. The cutoff can be implemented either in real space or in frequency space; in the latter case it is a high-frequency cutoff [23]. In either case, the modified function needs to be checked for permissibility. The covariance model (6) is plotted for $\alpha = 0.5$ in $R^2 \times T$ ($n = 2$) in Fig. 3A, and in $R^3 \times T$ ($n = 3$) in Fig. 3B. The shape of the covariance changes with the n- and α-values. Clearly, the same is true for the correlation ranges and the behavior near the space–time origin. Furthermore, starting from Eq. (6) with $n = 1$ and using Eq. (1) new covariance models can be found in $R^n \times T$ ($n = 2,3$) as follows

$$c_{X,n}(r,\tau) = B_n \int_0^1 \mathrm{d}u(1-u^2)^{(n-1)/2} \exp(-ur^2/4\alpha\tau), \tag{7}$$

where $B_n = (4\alpha\pi\tau)^{-1/2}E_n$. Recall that if a model is permissible in n dimensions, it is also permissible in n' dimensions, where $n' < n$. More specifically, in $R^2 \times T$ the Eq. (7) leads to the covariance model

$$c_{X,2}(r,\tau) = 0.125\pi^{1/2}(\alpha\tau)^{-1/2}E_2\ \mathrm{KummerM}[0.5, 2, -Z_A], \tag{8a}$$

where $Z_A = r^2(4\alpha\tau)^{-1}$, $\tau > 0$, and the KummerM($\cdot$) function is a solution to the Kummer's differential equation (see, Eq. (A.4) of Appendix). Model (8a) is plotted in Fig. 3C. In $R^3 \times T$, Eq. (7) yields the model

$$c_{X,3}(r,\tau) = 0.5r^{-1}E_3[(1 - 0.5Z_A^{-1})\mathrm{Erf}(Z_A^{1/2}) + (\pi Z_A)^{-1/2}\exp(-Z_A)] \tag{8b}$$

(r, $\tau > 0$). Eq. (8b) is plotted in Fig. 3D.

Other formulations as well as extensions of Eq. (6) are possible (in order to deal with the singularity at zero, to account for physical features of the underlying process etc.). Gneiting [18, p. 593] proposes space–time formulations which involve the addition of constants after the time lag. A similar approach was suggested by Hristopulos [22, p. 46] in the spatial case. In this way Eq. (6) may be modified, e.g., as follows

$$c_X(r,\tau) = (\beta\tau^{2\gamma} + 1)^{-n/2}\exp[-r^2/(\beta\tau^{2\gamma} + 1)] \tag{9a}$$

($0 \leqslant \beta \leqslant 1$, $0 < \gamma \leqslant 1$). The covariance class of Eq. (9a) has been used in fluid mechanics studies (e.g., [31, p. 156–160]). Certain generalizations of the form

$$c_X(r,\tau) = (B/(\tau - \zeta)^{\lambda})\phi(r^2/\chi(\tau - \zeta))$$

have also been investigated, where B, ζ, χ, and λ are physical coefficients and $\phi(\cdot)$ is a suitable function (see, [31, p. 161]). Starting from Eq. (9a) with $n = 1$, $\gamma = 0.5$, and applying the space transformation of Eq. (1) we find the new covariance models

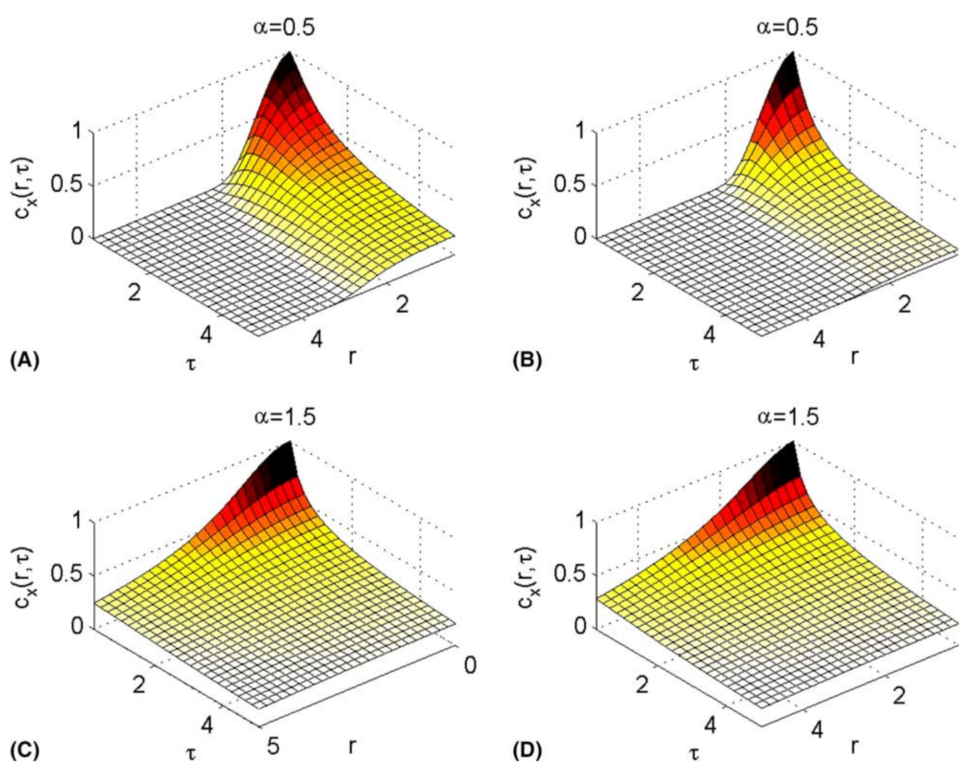

Fig. 3. Plots of the non-separable covariance model of Eq. (6) in the $R^2 \times T$ domain (plot A), in the $R^3 \times T$ domain (plot B), of the model (8a) (plot C) and of the model (8b) (plot D) for selected values of the parameter α.

$$c_{X,2}(r,\tau) = 0.25\pi(\beta\tau+1)^{-1/2}E_2\,\mathrm{KummerM}[0.5,2,-Z_B] \tag{9b}$$

and

$$c_{X,3}(r,\tau) = 0.5\pi^{1/2}r^{-1}E_3[(1-0.5Z_B^{-1})\mathrm{Erf}(Z_B^{1/2}) + (\pi Z_B)^{-1/2}\exp(-Z_B)], \tag{9c}$$

where $Z_B = r^2(\beta\tau+1)^{-1}$. Models (9b) and (9c) have been plotted in Fig. 4A and B, respectively, for selected values of the parameter β. Physical insight can lead to further extensions of the covariance class of Eq. (6) in the form of $c_X(r,\tau) \cong (b\tau)^{-m}\exp(-r^2/\alpha\tau)$, which includes the cases with $m = 0$ and $m > 1.5$ in $R^3 \times T$ (the coefficients m, a and b obtain physical meaning in the context of the turbulence study considered). Moreover, a series of non-separable spatiotemporal covariance models can be derived from Eq. (6), such as

$$c_X(r,\tau) = (1+b\tau^2)^{-3/2}[1-0.5r^2(1+b\tau^2)^{-1}] \times \exp[-0.5r^2/(1+b\tau^2)] \tag{10a}$$

and

$$c_X(r,\tau) = (1+b\tau^2)^{-5/2}\{1-r^2(1+b\tau^2)^{-1} + r^4[8(1+b\tau^2)^2]^{-1}\}\exp[-0.5r^2/(1+b\tau^2)]. \tag{10b}$$

Covariance models (10) in the $R^2 \times T$ domain are plotted in Fig. 4C and D for $b = 2$. Among the noticeable features of these plots is the presence of "hole effects", mainly, along the space direction.

It is worth mentioning that general pde can generate new classes of permissible spatiotemporal covariance functions based on other well-known functions. For example, Christakos [8, p. 184] used the physical pde, $D_{s,t}Z(s,t) = X(s,t)$ in $R^2 \times T$, where $s = (s_1, s_2)$ and $D_{s,t} = -a\partial^2/\partial t^2 + b(\partial^4/\partial s_1^4 + \partial^4/\partial s_2^4) + 2b\partial^4/\partial s_1^2\partial s_2^2$, to derive new spatiotemporal covariances $c_Z(\boldsymbol{r},\tau)$ starting from existing ones, $c_X(\boldsymbol{r},\tau)$, as follows

$$c_Z(\boldsymbol{r},\tau) = \int\int \mathrm{d}\boldsymbol{k}\mathrm{d}w\exp[\mathrm{i}(\boldsymbol{k}\cdot\boldsymbol{r}+w\tau)] \times (b\boldsymbol{k}^4+aw^2)^{-2}\tilde{c}_X(\boldsymbol{k},w), \tag{11}$$

where $\boldsymbol{r} = (r_1, r_2)$, $\boldsymbol{k} = (k_1, k_2)$, the a and b are positive coefficients, and $\tilde{c}_X(\boldsymbol{k},w)$ is the spectral density of $c_X(\boldsymbol{r},\tau)$. For illustration, we let $a = b = 1$ and use a spectral density of the form $\tilde{c}_X(\boldsymbol{k},w) = 2\pi\delta(w-\boldsymbol{k}\cdot\boldsymbol{v})$ $\exp(-\alpha^2\boldsymbol{k}^2/4)$, where $\boldsymbol{v}$ is a known parameter vector that represents a velocity vector (see, also, discussion in Section 2.2 below). Then, assuming spatial isotropy, Eq. (11) yields the following non-separable spatiotemporal covariance model in $R^2 \times T$,

$$c_Z(\boldsymbol{r},\tau) = 0.5\alpha\int_0^\infty \mathrm{d}k\,k^{-3}(k^2+v^2)^{-2} \times \exp(-\alpha^2\boldsymbol{k}^2/4)J_0[k(r+v\tau)], \tag{12}$$

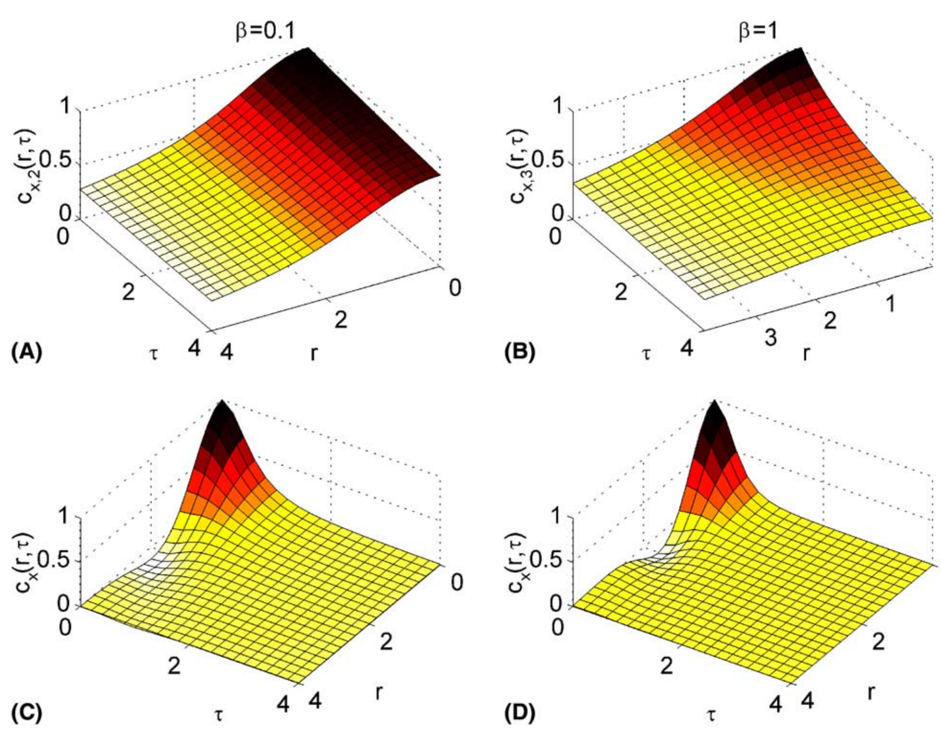

Fig. 4. The top row shows plots of the non-separable covariance model of Eq. (9b) (plot A) and of the model (9c) (plot B) for selected values of the parameter β. In the bottom row, plots of the non-separable covariance models of Eq. (10a) (plot C) and of Eq. (10b) (plot D) for the parameter value $b = 2$.

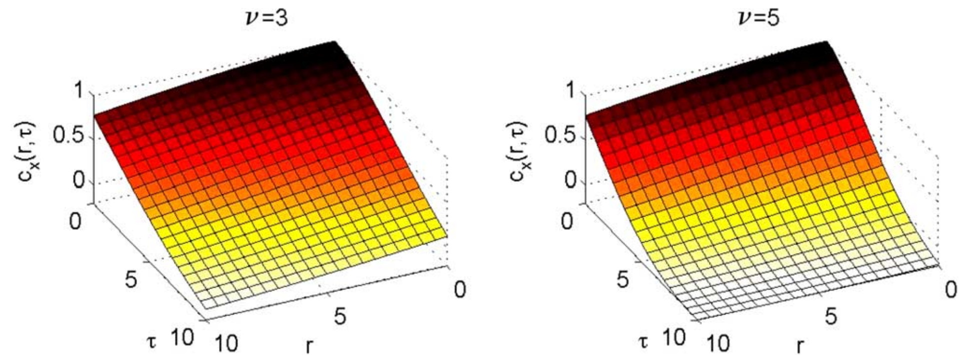

Fig. 5. Plots of the non-separable covariance model of Eq. (12) in the $R^2 \times T$ domain for $\alpha = 0.5$ and various values of ν.

where $v = \|\boldsymbol{v}\|$. Eq. (12) is calculated numerically leading to the covariance plot of Fig. 5 (shown for certain combinations of the α and v values). In a similar vein, starting from the physical pde $\mathscr{L}_{\boldsymbol{P}}[Z(\boldsymbol{p})] = X(\boldsymbol{p})$ in $R^n \times T$, where $\mathscr{L}_{\boldsymbol{P}} = (\partial/\partial t)\mathscr{L}_{\boldsymbol{S}}$, spatiotemporal covariance models can be generated by means of the equation

$$c_Z(\boldsymbol{p}, \boldsymbol{p}') = \int\int \mathrm{d}\boldsymbol{u}\,\mathrm{d}\boldsymbol{u}'\, c_X(\boldsymbol{u}, \boldsymbol{u}')g(\boldsymbol{p}, \boldsymbol{u})g(\boldsymbol{p}', \boldsymbol{u}'),$$

where g is the Green's function, which is the solution of $\mathscr{L}_{\boldsymbol{P}}[g(\boldsymbol{p}, \boldsymbol{u})] = \delta(\boldsymbol{p} - \boldsymbol{u})$. This process produces a versatile class of non-separable covariance models, not plotted in this work.

For certain applications, the *long-range* properties of the covariance functions are important. There is a class of covariance models with well-defined asymptotic behavior, while their dependence close to the origin is unspecified. For example, on the basis of the asymptotic correlation function for the noisy Burgers pde [17], an interesting non-separable covariance model $c_X(\boldsymbol{r}, \tau)$ for large r and τ values in $R^1 \times T$ is derived as follows [9, p. 226],

$$c_X(r, \tau) \cong A\sqrt{r^{z-2\alpha}\tau^{-1}}\exp(-r^{-z}\tau), \tag{13}$$

where $A = \exp(D/4)/4\sqrt{\pi D^3}$, and α, z, $D > 0$. The symbol "$\cong$" denotes that the covariance function is of this functional form for finite lags and asymptotically but not close to the origin. The shapes and the correlation ranges of model (13) depend on the parameters α and z. The magnitude of the slope increases with the ratio α/z.

2.2. Covariance models generated from spectral densities

A *spectral* method for generating covariance (and variogram) models of random fields was proposed in Christakos [4, p. 263–264]. One first constructs a suitable function in the wave-frequency domain (e.g., a spectral density) and then derives the covariance model in real space–time by applying an inverse transformation (Fourier or Hankel). This powerful method has been used extensively in the context of spatial as well as spatiotemporal analysis. A set of covariances associated with homogeneous/stationary random fields were derived by [25, p. 293–294] which have the spectral density $\tilde{c}_X(k, \omega) = [(k^2 + \alpha^2)^{2p} + c^2\omega^2]^{-1}$, where $p > n/2$. The corresponding covariance model in $R^n \times T$ is as follows

$$c_X(r, \tau) = \beta_n r^{1-n/2}\int_0^\infty \mathrm{d}k\, k^{n/2}\exp[-c^{-1}(k^2+\alpha^2)^p\tau] \times (k^2+\alpha^2)^{-p}J_{n/2-1}(kr), \tag{14}$$

where $\beta_n = [2(2\pi)^{n/2}c]^{-1}$ and $J_{n/2-1}$ denotes the Bessel function of the 1st kind and order $(n/2 - 1)$. We used numerical integration to calculate Eq. (14) for $p = n = 2$, which led to the covariance models in $R^2 \times T$ plotted in Fig. 6. In these plots the behavior of model (14) is examined for varying values of the parameters α and c. The covariance declines faster along the time direction than along the space direction.

In light of the space transformation analysis, another class of covariance models is generated by assuming a covariance given by Eq. (14) for $n = 1$ and then transforming it in higher dimensions by means of Eq. (1). This leads to the following double integral

$$c_{X,n}(r, \tau) = E_n\beta_n\int_0^1\int_0^\infty \mathrm{d}u\mathrm{d}k(1-u^2)^{(n-1)/2}(urk)^{1/2} \times \exp[-c^{-1}(k^2+\alpha^2)^p\tau](k^2+\alpha^2)^{-p}J_{-1/2}(kur), \tag{15}$$

where r, $\tau > 0$. In Fig. 6 we display examples of model (15) for $n = 3$, $c = 1$, 2, and $\alpha = 0.7$, 1.

Christakos [8, p. 185;9, p. 226–227] proposed a simple yet general δ-*technique* for constructing a rich class of non-separable spatiotemporal covariance models in $R^n \times T$, as follows. Assume a spectral density function in R^n, say $\tilde{c}_S(k)$, and let the corresponding density in $R^n \times T$ be $\tilde{c}_X(k, \omega) = 2\pi\delta(\omega \pm k \cdot v)\tilde{c}_S(k)$. Then, one can generate space–time covariance models as follows

$$c_X(\boldsymbol{r}, \tau) = (1/2\pi)^n\int \mathrm{d}\boldsymbol{k}\exp[\mathrm{i}(\boldsymbol{k}\cdot\boldsymbol{r} + \boldsymbol{v}\tau)]\tilde{c}_S(\boldsymbol{k}). \tag{16}$$

Note that if $\tilde{c}_S(k)$ is an isotropic spectral density, the frequency integral in Eq. (16) is simplified to an one-

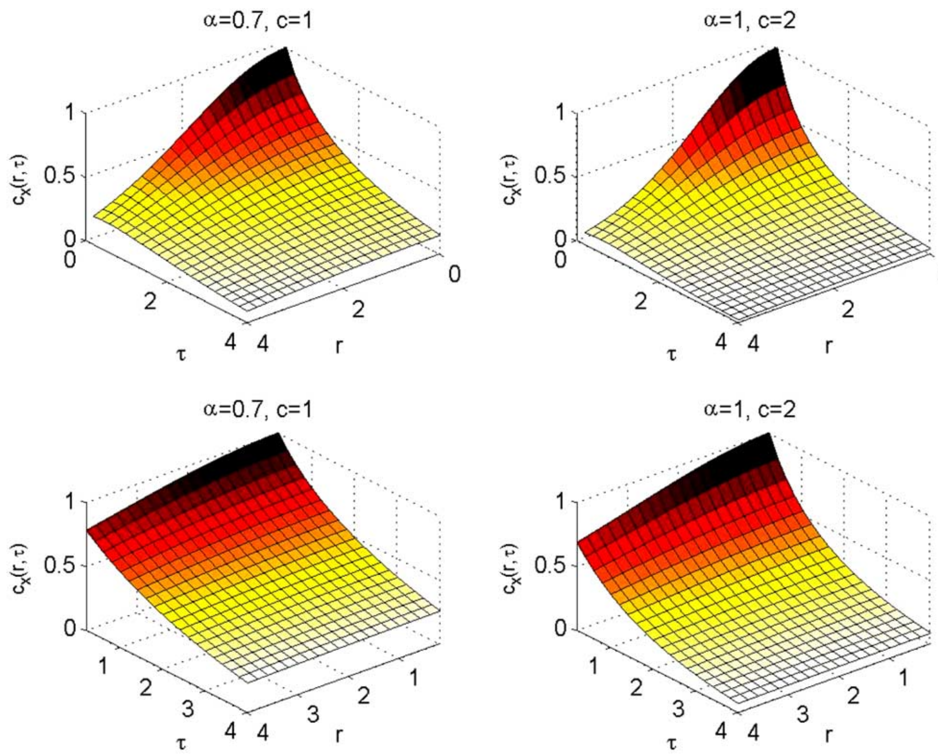

Fig. 6. Plots of the non-separable covariance models of Eq. (14) in the $R^2 \times T$ domain (top row) and of the model (15) in the $R^3 \times T$ domain (bottom row) for varying values of the parameters α and c.

dimensional integral over the magnitude of the frequency vector, which involves a Bessel function. The resulting one-dimensional integral is evaluated either explicitly or by numerical integration. If $\tilde{c}_S(k)$ has an inverse transform in R^n, say $c_X(\boldsymbol{r})$, then Eq. (16) reduces to $c_X(\boldsymbol{r},\tau) = c_s(\boldsymbol{r} \pm \boldsymbol{v}\tau)$, which implies that one can start with any of the covariance models $c_X(\boldsymbol{r})$ that are already available in the spatial statistics literature and simply use the equation above to obtain a permissible space–time covariance model. In this way, a variety of spatiotemporal covariance models can be generated from the corresponding purely spatial ones. A few examples are plotted next. In particular, consider the following spatiotemporal covariance models in $R^n \times T$

$$c_X(\boldsymbol{r},\tau) = \exp[-\|\boldsymbol{r} \pm \boldsymbol{v}\tau\|/\alpha], \tag{17}$$

and

$$c_X(\boldsymbol{r},\tau) = \exp[-(\boldsymbol{r} \pm \boldsymbol{v}\tau)^2/\alpha^2]. \tag{18}$$

These two models (17) and (18) are plotted in Fig. 7A and B, respectively (in the case of $\boldsymbol{r} + \boldsymbol{v}\tau$ and for selected combinations of α- and v-values). Furthermore, starting from the spatial covariance model $c_X(\boldsymbol{r}) = (1 + r^2/w^2)^{-v/2}$ $\exp(-\boldsymbol{r}/\xi)$ proposed by ([22] page 46), we obtained the following spatiotemporal model

$$c_X(\boldsymbol{r},\tau) = [1 + (\boldsymbol{r} \pm \boldsymbol{v}\tau)^2/w^2]^{-v/2} \exp[-\|\boldsymbol{r} \pm \boldsymbol{v}\tau\|/\xi]. \tag{19}$$

The model (19) is shown in Fig. 7C and D (for a positive sign of the space–time vector, $\boldsymbol{r} + \boldsymbol{v}\tau$), and for various combinations of the parameters v, w and ξ. Other spatiotemporal covariance models can be generated in a similar manner as Eqs. (17)–(19) above. Models of this kind can be useful in several physical applications, e.g., in cases in which the "frozen" random field hypothesis applies [32].

Another example of the spectral class is the following covariance model, which has been used in several applications in the $R^1 \times T$-domain (e.g., [8, p. 186],

$$c_X(r,\tau) = \exp\left(-\sqrt{r^2/a^2 + \tau^2/b^2}\right), \tag{20}$$

where a, $b > 0$ are coefficients corresponding to the spatial and temporal correlation scales. This model, which represents a homogeneous/stationary random field, is plotted in the upper half of Fig. 8. The behavior of model (20) in $R^1 \times T$ for small variations in the values of a and b is depicted in plots A and B of Fig. 8. It is worth noticing that, in view of the space transformation analysis of Eq. (2), the model (20) is permissible in $R^n \times T$ ($n = 2, 3$). Furthermore, using the space transformation approach of Eq. (1), novel spatiotemporal covariance models are obtained in $R^n \times T$ by means of the integral

$$c_{X,n}(r,\tau) = E_n \int_0^1 \mathrm{d}u(1-u^2)^{(n-1)/2} \times \exp\left(-\sqrt{(ur/a)^2 + (\tau/b)^2}\right). \tag{21}$$

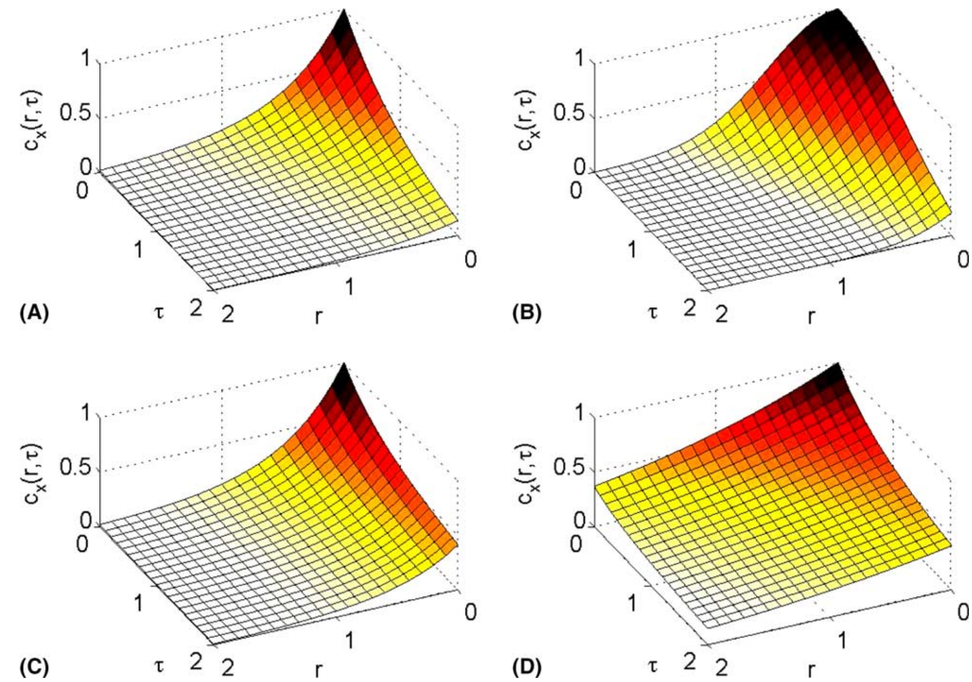

Fig. 7. Instances of the non-separable covariance models of Eq. (17) for $\alpha = 0.5$, $\nu = 0.5$ (plot A), the model of Eq. (18) for $\alpha = 0.8$, $\nu = 0.5$ (plot B), and the model of Eq. (19) in $R^n \times T$ ($n = 1,2,3$) shown in plot C for the parameter set $\nu = 1.5$, $w = 0.25$, $\xi = 0.5$, and in plot D for the parameter set $\nu = 1.5$, $w = 0.25$, $\xi = 2$.

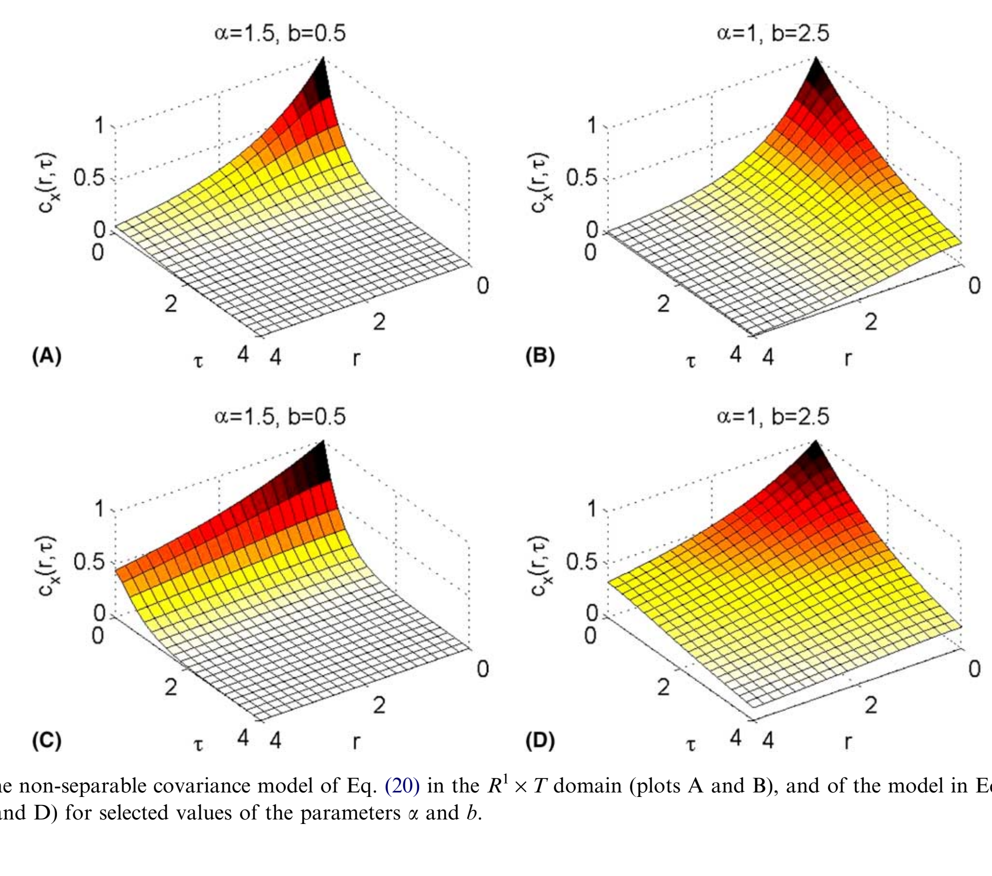

Fig. 8. Plots of the non-separable covariance model of Eq. (20) in the $R^1 \times T$ domain (plots A and B), and of the model in Eq. (21) in the $R^3 \times T$ domain (plots C and D) for selected values of the parameters α and b.

The corresponding functions are plotted in Fig. 8 (plots C and D).

2.3. Covariance models generated from dynamic rules

Another class of S/TRF is generated from *growth* and *pattern formation* processes in which there is a random element (e.g., a porous medium) and the spatiotemporal evolution is governed by a set of dynamic rules instead of a differential equation. A non-separable covariance model of this type that originates from simulations of invasion percolation satisfies the dynamic scaling form $c_X(r,\tau) \cong r^{-1}g(r^z/\tau)$, where z and $g(x)$ are suitable coefficient and function (for details, see [12, p. 113–114]). In this work we consider the case of

$$c_X(r,\tau) = \begin{cases} r^{\alpha z-1}/\tau^{\alpha}, & \text{if } r^z\tau^{-1} \ll 1, \\ \tau^{b}/r^{bz+1}, & \text{if } r^z\tau^{-1} \gg 1 \end{cases} \tag{22}$$

in $R^2 \times T$. A noticeable feature of Eq. (22) is that, under certain conditions, it can generate covariance models with ridges across space and time. Models with ridges along space or time have been discussed by Stein [35].

Fractal models exhibit a power-law asymptotic decay of the correlations with a non-integer exponent. The models can be fractal either in space (in which case the asymptotic behavior refers to $r \to \infty$) or in time (in which case the asymptotic behavior refers to $\tau \to \infty$). The following class of spatiotemporal covariance models in $R^n \times T$ has fractal properties over a corresponding space–time range

$$c_X(r,\tau) = \sigma^2 \hat{f}_z(\tau/r^{\beta}; u_c)\hat{f}_{\alpha}(r; w_c), \tag{23}$$

where $\hat{f}_v(r;u_c) = f_v(r;u_c)f_v^{-1}(0;u_c)$ and $f_v(r;u_c) = \Gamma^{-1}(-v)\int_0^{u_c} \mathrm{d}u \exp(-ur)u^{-(v+1)}$. As is shown in [14], the function $\hat{f}_z(\tau/r^{\beta};u_c)$ has an unusual dependence on the space and time lags through τ/r^{β}. For large τ and r, $\tau/r^{\beta} \to 0$ and $\hat{f}_z(\tau/r^{\beta};u_c) \to 1$. With regard to $\hat{f}_z(\tau/r^{\beta};u_c)$, two pairs of spatiotemporal points are "equidistant" if $\tau_1/r_1^{\beta} = \tau_2/r_2^{\beta}$ (in contrast with, e.g., a Gaussian spatiotemporal covariance function where equidistant lags satisfy the equation $r^2/\xi_r^2 + \tau^2/\xi_\tau^2 = c$). Permissibility conditions for the model (23) imply that $-1 < z < 0$ and $-(n+1)/2 < \alpha - \beta z < 0$ in R^n. These conditions can be relaxed by cutting off the short- and long-range behavior of the model, using the methods in [23]. A numerical illustration of the covariance model (23) in $R^n \times T$ is plotted in Fig. 9 for several values of the parameters z, β and α (note that a range of z- and β-values is assumed and the α is derived on the basis of the permissibility conditions above).

2.4. Covariance models obtained from generalized random field theory

Generalized spatiotemporal covariances, denoted as $\kappa_X(\boldsymbol{r},\tau)$, are often defined on the basis of the S/TRF theory of continuity orders ν in space and μ in time (S/TRF-ν/μ; [7, p. 861–875;8, p. 196–214]). Generalized covariances are associated with non-homogeneous/non-stationary data. Just as in the case of ordinary

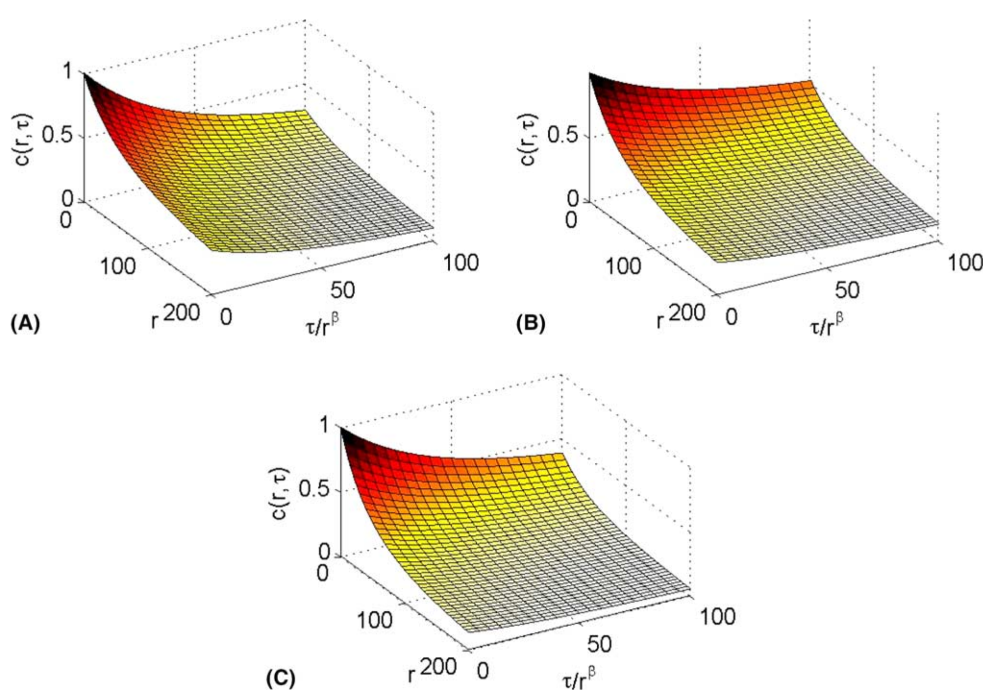

Fig. 9. Plots of the non-separable covariance model of Eq. (23) in the $R^n \times T$ domain for selected combinations of the parameters z, α, and β. In plot A: $z = -0.845$, $\alpha = -0.454$, $\beta = -0.35$. In plot B: $z = -0.385$, $\alpha = -0.615$, $\beta = -0.35$. In plot C: $z = -0.615$, $\alpha = -1.396$, $\beta = 1.05$.

covariances, generalized covariances can be derived from physical pde. Christakos and Hristopulos [12, p. 160–163] discuss certain illustrative examples. In one case, the corresponding equation of generalized covariances $\kappa_X(\mathbf{r},\tau)$ of the S/TRF-v/μ, $X(\mathbf{s},t)$, is as follows

$$(-1)^{v+\mu}(\nabla^2)^{v+1}\frac{\partial^{2\mu+2}}{\partial\tau^{2\mu+2}}\kappa_X(\mathbf{r},\tau) = c_Y(\mathbf{r},\tau), \tag{24}$$

where $\nabla^2 = \sum_{i=1}^{n}\partial^2/\partial r_i^2$ and c_Y is the ordinary centered covariance of a homogeneous/stationary field $Y(\mathbf{s},t)$ linked to the non-homogeneous/non-stationary field $X(\mathbf{s},t)$, through the physical pde.

A class of generalized covariance models which are solutions to Eq. (24) are of the following separable type

$$\kappa_X(r,\tau) = [G_1(r) + p_{2v+1}(r)][G_2(\tau) + p_{2\mu+1}(\tau)], \tag{25}$$

where the spatial and temporal kernels $G_1(r)$ and $G_2(\tau)$ are Green's functions in R^n defined as

$$G_1(r) = \begin{cases} r^{2v}\log r/[2^{2v+1}\pi(v!)^2], & n=2,\\ r^{2v-1}(-1)^{v+1}\Gamma(1/2-v)/(2^{2v+2}\pi^{3/2}v!), & n=3 \end{cases}$$

and

$$G_2(\tau) = (-1)^{\mu}\tau^{2\mu+1}\vartheta(\tau)/(2\mu+1)!.$$

Both the spatial v and temporal μ orders take the values 0, 1 or 2, in this case; $\vartheta(\tau)$ is the step function, i.e., $\vartheta(\tau) = 1$ if the temporal lag is $\tau > 0$ and $\vartheta(\tau) = 0$ otherwise. The spatial and temporal polynomials are, respectively, $p_{2v+1}(r) = \sum_{\rho=0}^{v}(-1)^{\rho}a_\rho r^{2\rho+1}$ and $p_{2\mu+1}(\tau) = \sum_{\zeta=0}^{\mu}(-1)^{\zeta}b_\zeta\tau^{2\zeta+1}$. Depending on the orders v and μ, certain permissibility conditions apply on the coefficients a_ρ and b_ζ (Table 1). Depending on the spatial dimension (R^2 vs. R^3) the coefficients c_i and d_i ($i = 0,1,2,3$) in Table 1 may assume different values as shown in Table 2. For illustration, the plots in Fig. 10 offer a comparative visualization of the generalized covariance model (25) in $R^3 \times T$ for different combinations of the orders v and μ (=0, 1 and 2).

Table 1
Permissibility conditions for the coefficients a_ρ and b_ζ

v, μ	a_ρ	b_ζ
0	$a_0 \geqslant 0$	$b_0 \geqslant 0$
1	$a_0, a_1 \geqslant 0$	$b_0, b_1 \geqslant 0$
2	$a_0, a_2 \geqslant 0$	$b_0, b_2 \geqslant 0$
	$a_1 \geqslant \frac{2}{c_1}\sqrt{a_0a_2c_0c_2}$	$b_1 \geqslant \frac{2}{d_1}\sqrt{b_0b_2d_0d_2}$

Table 2
Values of the coefficients c_i and d_i

	R^2	R^3
c_0, d_0	2π	8π
c_1, d_1	18π	96π
c_2, d_2	450π	2880π
c_3, d_3	$22\,050\pi$	$161\,280\pi$

A noticeable class of non-separable generalized covariances for non-homogeneous/non-stationary data is as follows

$$\begin{aligned}\kappa_X(r,\tau) = {}& \alpha_0\delta(r)\delta(\tau) + \delta(r)\sum_{\zeta=0}^{\mu}a_\zeta(-1)^{\zeta+1}\tau^{2\zeta+1}\\ &+ \delta(\tau)\sum_{\rho=0}^{v}b_\rho(-1)^{\rho+1}r^{2\rho+1}\\ &+ \sum_{\rho=0}^{v}\sum_{\zeta=0}^{\mu}d_{\rho/\zeta}(-1)^{\rho+\zeta}r^{2\rho+1}\tau^{2\zeta+1}\\ &+ \delta_{n,2}r^{2v}\log r\sum_{\zeta=0}^{\mu}(-1)^{\zeta}c_\zeta\tau^{2\zeta+1},\end{aligned} \tag{26}$$

where $\delta(r)$ and $\delta(\tau)$ are spatial and temporal delta functions, respectively; $\delta_{n,2}$ is Kronecker's delta; and α_0, a_ζ, b_ρ c_ζ, $d_{\rho/\zeta}$ are suitable coefficients. The first three terms in Eq. (26) represent discontinuities at the space–time origin; the fourth term is purely polynomial; the fifth term, which is logarithmic in the space lag, is obtained only in $R^2 \times T$. A representation of the general model (26) is plotted in Fig. 11, where we assumed that $\alpha_0 = a_\zeta = b_\rho = c_\zeta = 0$, $d_{0/0} = d_{2/1} = 1/4$, $d_{0/1} = 1/16$, $d_{1/0} = 1/2$, $d_{1/1} = 1/8$, and $d_{2/0} = 1$. Model (26) is useful for natural processes that have white noise residuals, $Y(\mathbf{s},t)$, but due to its simplicity it has been widely used in applied stochastics and modern spatiotemporal geostatistics. However, the assumption of white noise residual is restrictive, since more flexible models can be obtained using residuals with finite range correlations.

The power of the generalized S/TRF theory is demonstrated, among other things, by the fact that many useful models, like fractals and wavelets, are special cases of the generalized S/TRF theory (see [9, p. 251–259]). Furthermore, note that after the generalized covariance models (25) and (26) are constructed, ordinary non-homogeneous/non-stationary covariance models can be derived by means of the relationship

$$c_X(s,t;s',t') = \kappa_X(r,\tau) + p_{v/\mu}(s,t;s',t'), \tag{27}$$

where $p_{v/\mu}(s,t;s',t')$ are suitable space–time polynomials. In light of Eq. (27), even if one starts with a separable generalized function, like Eq. (25), the resulting ordinary covariance (27) is non-separable. Hence, equation (27) offers the means for generating a large class of potentially useful non-separable spatiotemporal covariance models, which can be used to represent spatially non-homogeneous/temporally non-stationary environmental processes and systems.

2.5. Covariance models constructed by linear superposition

It is well known that linear combinations of simple covariance models, $c_{x,i}$, are also valid covariance models

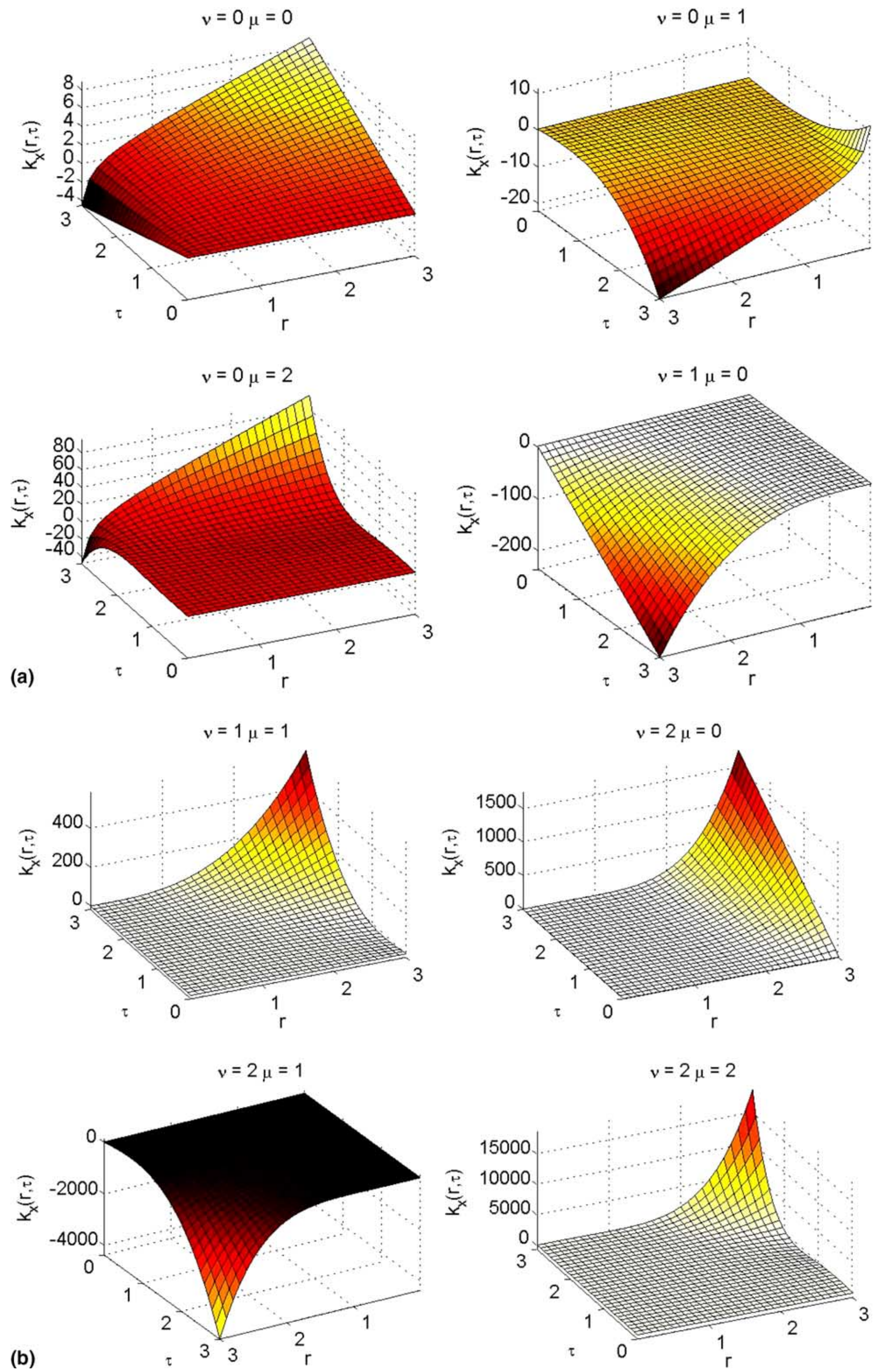

Fig. 10. Comparative plots of the generalized covariance model (25) in $R^3 \times T$ for pair values of the spatial and temporal continuity orders ν and μ, respectively.

$$c_X(\boldsymbol{r},\tau) = \sum_{j=1}^{N} \lambda_j c_{X,j}(\boldsymbol{r},\tau), \tag{28}$$

with weights $\lambda_j \geqslant 0$. The new covariance model c_X shares some of the features of the component models $c_{X,j}$ ($j = 1,\ldots,N$). However, the c_X can be a non-separable covariance model even if the components $c_{X,j}$ are separable space–time models. The simple but powerful statement of Eq. (28) is that we can combine the models discussed in the previous sections to produce

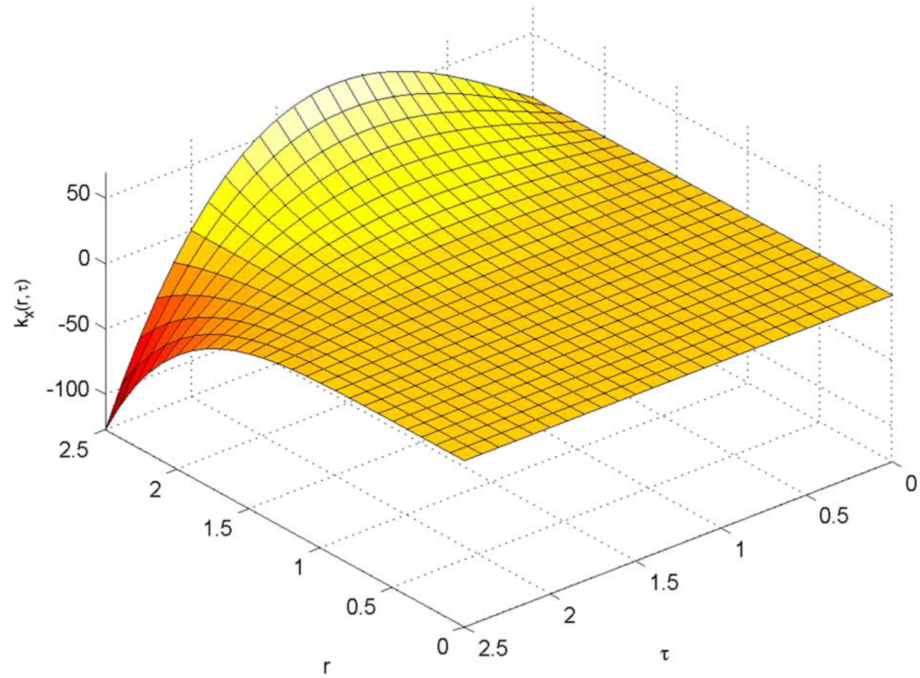

Fig. 11. Plot of a non-separable generalized covariance in the $R^2 \times T$ domain based on model (26).

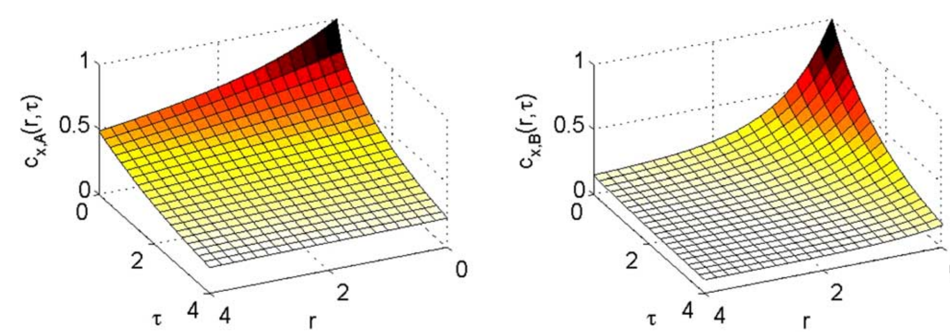

Fig. 12. Plots of non-separable covariances in the $R^2 \times T$ domain based on various linear combinations using models (4), (12), and (17).

new covariance models in space and time. For illustration, in Fig. 12 we plot covariance models of the form (28), where $N = 3$ and the component models $c_{X,j}$ ($j = 1, 2, 3$) are given by Eqs. (4), (12) and (17), respectively; various weight combinations λ_j ($j = 1, 2, 3$) are considered. Depending on the weights λ_j one can enhance or reduce the effect of the component models on the final covariance model (28). Indeed, in Fig. 12, the λ_2-value has been taken small enough compared to the λ_1- and λ_3-values in order to suppress the slow drop effect of $c_{X,2}$-component. In particular, $c_{X,A}$ is a combination of the weights $(\lambda_1, \lambda_2, \lambda_3) = (0.8, 0.1, 0.1)$, emphasizing the influence of model $c_{x,1}$; the neighboring plot of $c_{X,B}$ is created using $(\lambda_1, \lambda_2, \lambda_3) = (0.1, 0.1, 0.8)$, in which case the main contribution comes from the $c_{X,3}$-component.

3. Discussion

The variability of environmental processes is captured by the mean trend, which usually models "slow" variations of the process in space and time, and the (centered) covariance function, which incorporates "fast" variations of a seemingly random nature. The mean trend is typically determined from the equations of the physical laws that govern the process. If two fields are related by means of an equation (i.e., a pde) the fluctuations of the dependent field are related to the fluctuations of the independent field, and so are the respective covariance functions. The most straightforward example from stochastic hydrology is the problem of groundwater flow, in which the hydraulic head covariance is determined from the hydraulic conductivity covariance by means of the flow equations (i.e., Darcy's law and the continuity equation). Similar situations arise in space–time phenomena, in which the dynamic evolution of the process is typically governed by a set of pde or by means of dynamic "evolution" rules that are not amenable to a pde description.

In this work, rich classes of non-separable spatiotemporal covariance models are investigated for homogeneous/stationary as well as non-homogeneous/non-stationary data. These models cover a wide range of space–time correlation scenarios, which can be used to represent the variability of natural systems in space and time. We consider various methods for generating non-separable spatiotemporal covariance functions that include physical differential equations, spectral densities, dynamic rules, generalized random field theory, and linear superposition of permissible covariance functions. We have also discussed the use of scaling forms, which involve power-law combinations of space and time lags, and we have commented on the need for truncating the power-law models at short and long range, in order to obtain permissible covariance functions. As is shown in the space–time plots of the covariance models above, the different scenarios lead to distinct features. Hence, the visual representation of the covariance models is very helpful in selecting the appropriate model for the specific physical situation. The covariance models presented here are based on general and powerful composite space–time random field theories, which deserve further attention by the communities engaged in spatiotemporal statistics research.

Acknowledgments

We would like to thank the referees for their valuable time and suggestions. We acknowledge the support for this work provided by the National Institute of Environmental Health Sciences (Grants P42-ES05948 and P30-ES10126).

Appendix I. We define the Fourier transform (FT) of the covariance function $c_{X,n}(\boldsymbol{r},\tau)$, i.e., the covariance spectral density, by means of the following integral in the $R^n \times T$ domain ($n = 1,2,3$)

$$\tilde{c}_{X,n}(\boldsymbol{k},\omega) = \int\int \mathrm{d}\boldsymbol{r}\,\mathrm{d}\tau\,\mathrm{e}^{-\mathrm{i}(\boldsymbol{kr}+\omega\tau)} c_{X,n}(\boldsymbol{r},\tau). \tag{A.1}$$

Then, the inverse Fourier transform determines the covariance function from the spectral density of the covariance as follows

$$c_{X,n}(\boldsymbol{r},\tau) = (2\pi)^{-n-1}\int\int \mathrm{d}\boldsymbol{k}\,\mathrm{d}\omega\,\mathrm{e}^{\mathrm{i}(\boldsymbol{kr}+\omega\tau)}\tilde{c}_{X,n}(\boldsymbol{k},\omega). \tag{A.2}$$

II. The complementary error function is defined as

$$\mathrm{Erfc}(x) = \begin{cases} (2/\sqrt{\pi})\int_x^\infty \mathrm{d}v\exp(-v^2), & \text{if } x \geqslant 0,\\ 2 - \mathrm{Erfc}(-x), & \text{if } x < 0. \end{cases} \tag{A.3}$$

III. The KummerM(a,b,z) function is a solution to the Kummer's differential equation

$$z\frac{\mathrm{d}^2 w}{\mathrm{d}z^2} + (b-z)\frac{\mathrm{d}w}{\mathrm{d}z} - aw = 0 \quad [1, \text{Chapter } 13]. \tag{A.4}$$

The KummerM function can be written in the power series form

$$\mathrm{KummerM}(a,b,z) = 1 + \frac{az}{b} + \cdots + \frac{(a)_n z^n}{(b)_n n!} + \cdots, \tag{A.5}$$

where $(a)_n = a(a+1)\cdots(a+n-1)$ with $(a)_0 = 1$.

References

[1] Abramowitz M, Stegun IA. Handbook of mathematical functions. New York, NY: Dover Publications, Inc.; 1972.
[2] Bogaert P. Geostatistics applied to the analysis of space–time data. PhD thesis. Universite Catholique de Louvain, Louvain-la-Neuve, Belgium, 1996.
[3] Bogaert P, Christakos G. Spatiotemporal analysis and processing of thermometric data over Belgium. J Geophys Res 1997; 102(D22):25,831–46.
[4] Christakos G. On the problem of permissible covariance and variogram models. Water Resour Res 1984;20(2):251–65.
[5] Christakos G. The space transformations and their applications in systems modelling and simulation. In: 12th International Conference, Athens Greece, AMSE, vol. 1(3), 1984. p. 49–68.
[6] Christakos G. Space transformations in the study of multidimensional functions in the hydrologic sciences. Adv Water Resour 1986;9(1):42–8.
[7] Christakos G. On certain classes of spatiotemporal random fields with applications to space–time data processing. IEEE Trans Syst Man Cybernet 1991;21(4):861–75.
[8] Christakos G. Random field models in earth sciences. San Diego, CA: Academic Press; 1992 (out of print). New edition, Mineola, NY: Dover Publ. Inc.; 2004.
[9] Christakos G. Modern spatiotemporal geostatistics. New York, NY: Oxford University Press; 2000.
[10] Christakos G, Bogaert P. Spatiotemporal analysis of springwater ion processes derived from measurements at the Dyle Basin in Belgium. IEEE Trans Geosci Remote Sensing 1996;34(3):626–42.
[11] Christakos G, Raghu VR. Dynamic stochastic estimation of physical variables. Math Geol 1996;28(3):341–65.
[12] Christakos G, Hristopulos DT. Spatiotemporal environmental health modelling: a Tractatus Stochasticus. Dordrecht, The Netherlands: Kluwer Acad. Publ.; 1998.
[13] Christakos G, Serre ML. BME analysis of spatiotemporal particulate matter distributions in North Carolina. Atmosph Environ 2000;34(20):3393–406.
[14] Christakos G, Hristopulos DT, Bogaert P. On the physical geometry concept at the basis of space/time geostatistical hydrology. Adv Water Res 2000;23:799–810.
[15] Christakos G, Bogaert P, Serre ML. Temporal GIS. New York, NY: Springer-Verlag; 2002, 20p, With Cd-Rom.
[16] Cressie N, Huang H-C. Classes of nonseparable spatio-temporal stationary covariance functions. J Am Statist Assoc 1999;94: 1330–40.

[17] Fogedby HC. Morphology and scaling in the noisy Burgers equation: soliton approach to the strong coupling fixed point. Phys Rev Lett 1998;80(6):1126–9.

[18] Gneiting T. Nonseparable, stationary covariance functions for space–time data. J Am Statist Assoc 2002;97(458):590–600.

[19] Goovaerts P, Sonnet P. Study of spatial and temporal variations of hydrogeochemical variables using factorial kriging analysis. In: Soares A, editor. Geostatistics Troia'92, vol. 2, 1993. p. 745–56.

[20] Handcock MS, Wallis JR. An approach to statistical spatial–temporal modeling of meteorological fields. J Am Statist Assoc 1994;89(426):368–90.

[21] Heine V. Models for two-dimensional stationary stochastic processes. Biometrica 1955;42:170–8.

[22] Hristopulos DT. New anisotropic covariance models and estimation of anisotropic parameters based on the covariance tensor identity. Stochast Environ Res Risk Assess 2002;16:43–62.

[23] Hristopulos DT. Permissibility of fractal exponents and models of band-limited two-point functions for fGn and fBm random fields. Stochast Environ Res Risk Assess 2003;17:191–216.

[24] Hristopulos DT. Anisotropic Spartan random field models for geostatistical analysis. In: Agioutantis Z, Komnitsas K, editors. Proceedings of Advances in Mineral Resources Management and Environmental Geotechnology. Heliotopos Conferences, Athens, Greece, 2004.

[25] Jones RH, Zhang Y. Models for continuous stationary space–time processes. In: Gregoire TG, Brillinger DR, Diggle PJ, Russek-Cohen E, Warren WG, Wolfinger RD, editors. Modelling longitudinal and spatially correlated data. New York, NY: Springer-Verlag; 1997. p. 289–98.

[26] Kyriakidis PC, Journel AG. Geostatistical space–time models: A review. Math Geol 1999;31:651–84.

[27] Ma C. Spatio-temporal covariance functions generated by mixtures. Math Geol 2002;34(8):965–75.

[28] Ma C. Spatio-temporal stationary covariance models. J Multivariate Anal 2003;86:97–107.

[29] Ma C. Families of spatio-temporal stationary covariance models. J Statist Planning Infer 2003;116:489–501.

[30] Mardia KV, Goodall C, Redfern E, Alonso FJ. The kriged Kalman filter. Test 1998;7:217–85.

[31] Monin AS, Yaglom AM. Statistical fluid mechanics, vol. 2. Cambridge, MA: The MIT Press; 1975.

[32] Pope SB. Turbulent flows. Cambridge, U.K: Cambridge University Press; 2000.

[33] Posa D. A simple description of spatial–temporal processes. Comput Statist 1993;15(4):425–38.

[34] Rubin Y. Applied stochastic hydrogeology. New York, NY: Oxford University Press; 2002.

[35] Radon J. Über die Bestimmung von Funktionen durch ihre Integralwerte längs gewisser Mannigfaltigkeiten, Ber Verh Sächs Akad Wiss Leipzig, Math-Phys Klasse 1917;69:262–277.

[36] Stein M. Space–time covariance functions. Technical Rep. 4, Center for Integrating Statistical and Environ Science, University of Chicago, IL, 2004.

[37] Vyas V, Christakos G. Spatiotemporal analysis and mapping of sulfate deposition data over the conterminous USA. Atmosph Environ 1997;31(21):3623–33.